High pressure elastic properties of minerals from ab initio simulations: The case of pyrope, grossular and andradite silicate garnets.

(Article begins on next page)

19 November 2024

A. Erba, A. Mahmoud, D. Belmonte, R. Dovesi
High pressure elastic properties of minerals from ab initio simulations: The case of pyrope, grossular and andradite silicate garnets.

High Pressure Elastic Properties of Minerals from Ab initio Simulations: The Case of Pyrope, Grossular and Andradite Silicate Garnets.

A. Erba,[1, a)] A. Mahmoud,[1] D. Belmonte,[2] and R. Dovesi[1]

[1)] *Dipartimento di Chimica and Centre of Excellence NIS (Nanostructured Interfaces and Surfaces),*
Università di Torino, via Giuria 5, IT-10125 Torino (Italy)

[2)] *DISTAV, Università di Genova, Corso Europa 26, 16132 Genoa, Italy*

A computational strategy is devised for the accurate *ab initio* simulation of elastic properties of crystalline materials under pressure. The proposed scheme, based on the evaluation of the analytical stress tensor and on the automated computation of pressure-dependent elastic stiffness constants, is implemented in the CRYSTAL solid state quantum-chemical program. Elastic constants and related properties (bulk, shear and Young moduli, directional seismic wave velocities, elastic anisotropy index, Poisson's ratio, etc.) can be computed for crystals of any space group of symmetry. We apply such a technique to the study of high-pressure elastic properties of three silicate garnet end-members (namely, pyrope, grossular and andradite) which are of great geophysical interest, being among the most important rock-forming minerals. The reliability of this theoretical approach is proved by comparing with available experimental measurements. The description of high-pressure properties provided by several equations of state is also critically discussed.

I. INTRODUCTION

The elastic properties of the Earth's crust, mantle and transition zone, that can be measured by modern seismological techniques, constitute a reliable ground on which different geological compositional models can be discussed.[94] A obvious prerequisite to this discussion, is the knowledge of the elastic properties of the main minerals and rocks which constitute the Earth's interior, at geophysical (*i.e.* high pressure, high temperature) conditions. A complete characterization of the elastic properties of a material is given in terms of its elastic constants, from which seismic wave propagation velocities, and bulk, shear and Young moduli can be deduced.[95–98]

In the last decades, an enormous amount of X-ray diffraction studies were performed which measured isothermal equations of state of several rock-forming minerals in order to determine their equilibrium bulk modulus K_0 and its pressure derivative K_0'.[99] Experimental measurements of elastic constants under pressure are by far less frequent. At ambient pressure, different experimental determinations of K_0 agree relatively well to each other. However, when the high-pressure elastic behavior is considered, deviations up to 50 % have been reported as regards K_0'. As Jiang *et al.*[100] correctly pointed out, the magnitude of these discrepancies is such to prevent any reliable geological interpretation of seismic data.

We have recently shown how accurately *ab initio* simulations can predict reliable elastic properties of a family of silicate garnets, among the most important rock-forming minerals, at ambient pressure.[101,102] In this contribution, we consider the much more ambitious task of proving the reliability of theoretical simulations in predicting high-pressure, up to 60 GPa, elastic properties of minerals of

geophysical interest. Some members of the same family of garnets are considered. In order to do so, we have implemented a number of algorithms into the public CRYSTAL program that are described into some detail in Section II.

Beside their geological interest, garnets are technologically relevant materials as components of lasers, computer memories, microwave optical devices and as abrasives and filtration media.[103] Silicate garnets, in particular, are among the main constituents of the Earth's lower crust, upper mantle and transition zone. They exhibit a cubic structure (space group $Ia\overline{3}d$) and formula $X_3Y_2(SiO_4)_3$, where the X site hosts divalent cations such as Ca^{2+}, Mg^{2+}, Fe^{2+} and Mn^{2+} and the Y site is occupied by trivalent cations such as Al^{3+}, Fe^{3+} and Cr^{3+}.[104] Their primitive cell contains 80 atoms, that correspond to four formula units. Among the most common end-members of the family, here we consider pyrope $Mg_3Al_2(SiO_4)_3$, grossular $Ca_3Al_2(SiO_4)_3$ and andradite $Ca_3Fe_2(SiO_4)_3$.

Few Brillouin scattering experimental measurements exist of the elastic constants under pressure of these minerals: two studies for pyrope,[105,106] two for grossular,[100,106] and two for andradite.[106,107] From a theoretical perspective, few simulations using empirical/semiempirical potentials have been performed on the elastic properties of garnets at ambient pressure.[108–110] Beside our recent investigation of the ambient pressure elastic properties of six end-members (pyrope, grossular, andradite, spessartine, uvarovite and almandine),[101,102] only other two *ab initio* studies are reported: Li *et al.*[111] performed molecular dynamics simulations of the elastic constants of pyrope, as a function of pressure and temperature, in a projector-augmented-waves (PAW) density-functional-theory (DFT) implementation; Kawai and Tsuchiya[112] performed DFT calculations of the elastic properties of grossular, in the local-density approximation (LDA).

a)Electronic mail: alessandro.erba@unito.it

In this paper, we report a full set of elastic properties of pyrope, grossular and andradite at high-pressure, computed *ab initio* using a fully periodic implementation of the hybrid B3LYP, Becke-three parameters-Lee-Yang-Parr,[113,114] functional and all-electron basis sets. The possibility of using all-electron basis sets instead of pseudo-potentials describing core electrons has recently been shown to be of particular relevance when calculations under pressure are performed since also core electrons can participate to the chemical bonding.[115] The same computational approach was successfully applied to the investigation of structural, electronic, vibrational (Infrared and Raman), magnetic, optical and elastic (at ambient pressure) properties of silicate garnets.[101,116–122] Calculations are performed with a development version of the CRYSTAL14 program[123] where a fully-automated and general procedure for computing elastic and piezoelectric tensors, photoelastic constants and seismic velocities of crystals of any symmetry has recently been implemented and applied to the study of several crystals.[101,124–130]

The paper is organized as follows: in Section II we present the theoretical techniques that we have developed and implemented in the CRYSTAL program for dealing with the effect of pressure, such as an automated algorithm for the computation of various equations of state, the calculation of the analytical stress tensor and the pressure dependence of elastic stiffness constants; Section III is devoted to the definition of the adopted computational setup; our results, as compared with available experimental data, are discussed in Section IV as regards the pressure-volume relation, and pressure dependence of the elastic constants and bulk modulus; conclusions are drawn in Section V.

II. THEORETICAL TECHNIQUE

This Section is devoted to the description of the theoretical procedure that we have set up, and implemented in the CRYSTAL program, for computing elastic properties of crystals of any space group of symmetry at high pressure, at the *ab initio* level. A fully analytical scheme, based on the stress tensor, is used for optimizing the proper volume associated with a given pressure, as described in Section II A. Alternatively, an equation of state could be used (see Section II B); as we shall discuss in the next section, however, the former approach is preferable as it is more accurate. The elastic properties under hydrostatic pressure are then computed at the corresponding volume, according to the methodology described in Section II C.

A. P-V Relation through Analytical Stress Tensor

The stress tensor $\boldsymbol{\sigma}$ is a symmetric second-rank tensor that can be computed analytically from the total energy

density derivatives with respect to strain:

$$\sigma_{ij} = \frac{1}{V} \frac{\partial E}{\partial \epsilon_{ij}} = \frac{1}{V} \sum_{k=1}^{3} \frac{\partial E}{\partial a'_{ki}} a_{kj} , \qquad (1)$$

with $\boldsymbol{\epsilon}$ second-rank symmetric pure strain tensor and $i, j = x, y, z$. In the second equality, $\partial E / \partial \epsilon_{ij}$ has been expressed in terms of analytical energy gradients with respect to lattice parameters, with a_{ij} elements of a 3×3 matrix, $\mathbf{A}$, where Cartesian components of the three lattice vectors $\mathbf{a}_1$, $\mathbf{a}_2$ and $\mathbf{a}_3$ are inserted by rows [$V = \mathbf{a}_1(\mathbf{a}_2 \times \mathbf{a}_3)$ is the cell volume]; when a distortion is applied to the cell, the lattice parameters transform as

$$a'_{ij} = \sum_{k=1}^{3} (\delta_{jk} + \epsilon_{jk}) a_{ik} , \qquad (2)$$

where δ_{jk} is the Kronecker delta. The difficult part of the calculation of the stress tensor in equation (1) is the evaluation of the analytical energy gradients with respect to the cell parameters, which have been implemented in the CRYSTAL program about ten years ago by Doll *et al.* for 1D, 2D and 3D periodic systems. Details about the implementation and the explicit form of the internal energy E can be found in Refs. 131 and 132.

An external "pre-stress" in the form of a hydrostatic pressure P,

$$\sigma_{ij}^{\text{pre}} = P \delta_{ij} , \qquad (3)$$

can be added to that of equation (1). Given that the optimizer works in terms of analytical cell gradients, in order to perform a pressure-constrained geometry optimization, the total stress tensor has to be back-transformed to obtain the corresponding constrained gradients:

$$\frac{\partial H}{\partial a_{ij}} = \frac{\partial E}{\partial a_{ij}} + PV(\mathbf{A}^{-1})_{ji} . \qquad (4)$$

Let us note that, with the inclusion of a hydrostatic pressure, the function to be minimized becomes the enthalpy $H = E + PV$. The implementation of a geometry optimizer under an external hydrostatic pressure, in the CRYSTAL program, has been done by Doll.[133] so that the optimized volume V of any crystal at a given hydrostatic pressure P can be computed analytically.

B. P-V Relation through Equation of State

An alternative approach for establishing the *P-V* relation of a crystalline material is using so-called Equations of State (EOS). The "cold" EOS is an energy-volume or pressure-volume relation which describes the behavior of a solid under compression and expansion, at $T = 0$ K, that is the case of standard *ab initio* simulations. Universal, *i.e.* not specific of particular materials, EOSs are usually expressed as analytical functions of a limited set of parameters (equilibrium energy

E_0, equilibrium volume V_0, equilibrium bulk modulus $K_0 = -V\partial P/\partial V$ and pressure derivative of equilibrium bulk modulus $K'_0 = \partial K_0/\partial P)$ for ease of interpolation, extrapolation and differentiation, and are quite used in solid state physics and geophysics.[134,135]

The main purpose EOSs are commonly used for, in theoretical simulations, is passing from (few) energy-volume data in the vicinity of the equilibrium volume to the P-V relation and, possibly, to high-pressure properties. To do so, energy-volume data are numerically fitted to the analytical $E(V)$ functional form of the EOS. From $P = -\partial E/\partial V$, the P-V connection is established. In principle, an advantage of this approach would be the possibility of predicting the high-pressure behavior of a solid from low-pressure or even equilibrium properties: the explicit dependence of the bulk modulus on volume (or pressure from P-V), is given by $K(V) = V\partial^2 E/\partial V^2$. Let us recall that the analytical expression of the $E(V)$ relation is generally obtained as a series which is truncated to some order. By taking derivatives of increasing order of this expression, for computing pressure P, bulk modulus K and its pressure derivative K', the error introduced by that truncation increases. This is particularly so when EOSs are used for extrapolating to high pressures.

A number of universal EOSs have been proposed so far.[134,136–141] All of them are phenomenological and can behave quite differently from each other as regards extrapolation at high pressure. Comprehensive reviews and comparisons of different EOSs are available in the literature.[142–146] Four EOSs are currently implemented in the CRYSTAL14 program: the original third-order Murnaghan's,[136] the third-order Birch's,[137,138] the logarithmic Poirier-Tarantola's,[141] and the exponential Vinet's.[139] In Appendix A, we report the explicit functional form of these EOSs and, in particular, of the corresponding expressions for the bulk modulus dependence on volume. A discussion on how they differently perform in extrapolating P-V and K-V relations up to the high-pressure regime for silicate garnets will be given in Section IV.

C. Elastic Properties at P > 0

In the absence of any finite pre-stress, elastic constants can be defined as second energy density derivatives with respect to pairs of infinitesimal Eulerian strains:

$$C_{ijkl} = \frac{1}{V_0}\left(\frac{\partial^2 E}{\partial \epsilon_{ij}\partial \epsilon_{kl}}\right)_{\epsilon=0}. \qquad (5)$$

The constants above do represent the link between stress and strain via the Hooke's law. In the limit of zero temperature, typical of *ab initio* simulations, they are also referred to as athermal elastic constants. For details about the implementation of the elastic tensor calculation in the CRYSTAL program see Refs. 101 and 124.

If a finite pre-stress $\boldsymbol{\sigma}^{\mathrm{pre}}$ is applied in the form of a hydrostatic pressure P, as in equation (3), within the frame of finite Eulerian strain, the relevant elastic stiffness constants read:[97,147–150]

$$B_{ijkl} = C_{ijkl} + \frac{P}{2}(2\delta_{ij}\delta_{kl} - \delta_{il}\delta_{jk} - \delta_{ik}\delta_{jl}), \qquad (6)$$

provided that V_0 in equation (5) becomes the equilibrium volume $V(P)$ at pressure P. In the present, fully automated, implementation of the calculation of the stiffness tensor $\mathbf{B}$ (and of $\mathbf{S} = \mathbf{B}^{-1}$, the compliance tensor) under pressure, $V(P)$ is obtained from the analytical stress tensor described in Section II A. An option exists for using the $V(P)$ relation obtained from a given EOS, as discussed in Section II B.

Since both $\boldsymbol{\epsilon}$ and $\boldsymbol{\delta}$ are symmetric tensors, we can rewrite the equality (6) as:

$$B_{vu} = C_{vu} + \begin{pmatrix} 0 & P & P & 0 & 0 & 0 \\ P & 0 & P & 0 & 0 & 0 \\ P & P & 0 & 0 & 0 & 0 \\ 0 & 0 & 0 & \frac{-P}{2} & 0 & 0 \\ 0 & 0 & 0 & 0 & \frac{-P}{2} & 0 \\ 0 & 0 & 0 & 0 & 0 & \frac{-P}{2} \end{pmatrix}, \qquad (7)$$

where Voigt's notation has been used, according to which $v, u = 1, \ldots 6$ ($1 = xx$, $2 = yy$, $3 = zz$, $4 = yz$, $5 = xz$, $6 = xy$).[151] The elastic stiffness tensor exhibits, in general, 21 independent elements that reduce to 3 (*i.e.* B_{11}, B_{12} and B_{44}) for crystals with cubic symmetry, as in the case here considered of silicate garnets.

High-pressure elastic properties of isotropic polycrystalline aggregates can be computed from the elastic stiffness and compliance constants defined above via the Voigt-Reuss-Hill averaging scheme.[152] In particular, for cubic crystals, the adiabatic bulk modulus K_0 is simply defined as:

$$K_0 = \frac{1}{3}(B_{11} + 2B_{12}) \equiv \frac{1}{3}(S_{11} + 2S_{12})^{-1}. \qquad (8)$$

The shear modulus $\overline{G} = 1/2[G_V + G_R]$ can be expressed as the average between Voigt upper G_V and Reuss lower G_R bounds as:

$$\overline{G} = \frac{1}{10}(B_{11} - B_{12} + 3B_{44}) + \frac{5}{2}(4(S_{11} - S_{12}) + 3S_{44})^{-1}.$$

From the bulk modulus and the average shear modulus defined above, Young's modulus E and Poisson's ratio σ can be defined as well:

$$E = \frac{9K_0\overline{G}}{3K_0 + \overline{G}} \quad \text{and} \quad \sigma = \frac{3K_0 - 2\overline{G}}{2(3K_0 + \overline{G})}. \qquad (9)$$

A further elastic property of great interest is the so-called elastic wave anisotropy which can be measured by the dimensionless parameter A that vanishes for an isotropic material.[153,154] For cubic crystals, seismic wave velocities along high symmetry directions can be computed with simple analytical expressions in terms of the

elastic stiffness constants;[155] as a consequence, the elastic wave anisotropy A can be given the following simple form:

$$A = \left[\frac{2B_{44} + B_{12}}{B_{11}} - 1\right] \times 100 \, . \qquad (10)$$

Even cubic crystals show non-zero elastic wave anisotropy.

III. COMPUTATIONAL DETAILS

All the calculations reported in this manuscript are performed with the CRYSTAL14 program for *ab initio* quantum physics and chemistry of solid state.[123] The B3LYP one-electron Hamiltonian is adopted, which contains a hybrid Hartree-Fock/Density-Functional exchange-correlation term. All-electron atom-centered Gaussian-type-function (GTF) basis sets are adopted. Oxygen atoms are described by a $(8s)$-$(411sp)$-$(1d)$ contraction of primitive GTFs, silicon by a $(8s)$-$(6311sp)$-$(1d)$ one, aluminum by a $(8s)$-$(611sp)$-$(1d)$ one, calcium by a $(8s)$-$(6511sp)$-$(21d)$ one and magnesium by a $(8s)$-$(511sp)$-$(1d)$ one. For iron, a $(8s)$-$(64111sp)$-$(411d)$ contraction of GTFs is used, augmented with a further f-type polarization function as reported into details in previous works.[117,118,156]

In CRYSTAL, the truncation of infinite lattice sums is controlled by five thresholds, which are set to 7 7 7 7 16.[157] Reciprocal space is sampled according to a sublattice with shrinking factor 3, corresponding to 4 points in the irreducible Brillouin zone. The DFT exchange-correlation contribution is evaluated by numerical integration over the cell volume: radial and angular points of the atomic grid are generated through Gauss-Legendre and Lebedev quadrature schemes, using an accurate predefined pruned grid: the accuracy in the integration procedure can be estimated by evaluating the error associated with the integrated electronic charge density in the unit cell versus the total number of electrons per cell: $2 \times 10^{-5}|e|$ out of a total number of 800 electrons per cell for pyrope, for instance. The convergence threshold on energy for the self-consistent-field (SCF) step of the calculations is set to 10^{-10} hartree.

Equilibrium and strained configurations are optimized by use of analytical energy gradients calculated with respect to both atomic coordinates and unit-cell parameters or atomic coordinates only, respectively.[158–160] A quasi-Newtonian technique is used, combined with the BFGS algorithm for Hessian updating.[161–164] Convergence is checked on both gradient components and nuclear displacements; the corresponding tolerances on their root mean square are chosen to be 10 times more severe than the default values for simple optimizations: 0.00003 a.u. and 0.00012 a.u., respectively. For the elastic constants calculation, two strained configurations are considered for each independent strain, with a dimensionless strain amplitude of 0.01.
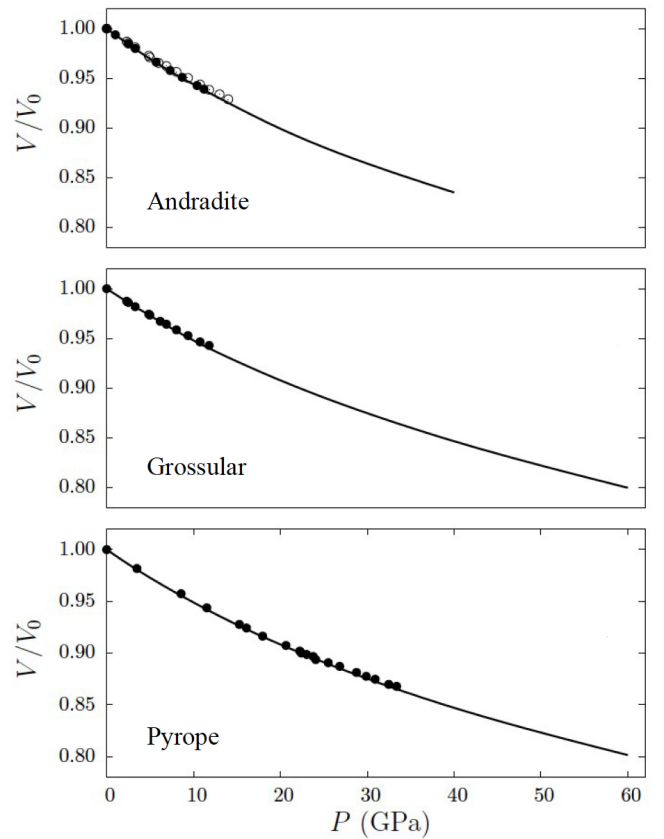

FIG. 1. For each garnet (andradite in the upper panel, grossular in the middle panel and pyrope in the lower panel), V/V_0 is reported as a function of pressure P. Continuous lines represent computed values as fitted with a cubic spline. Computed values are obtained with the analytical stress tensor scheme at 8 pressures in the range 0 GPa - 60 GPa for pyrope and grossular and at 7 pressures in the rage 0 GPa - 40 GPa for andradite, as reported in Table I. Circles are experimental data from Ref. 165 for pyrope, Ref. 166 for grossular and Ref. 107 (full circles) and 166 (empty circles) for andradite.

IV. RESULTS AND DISCUSSION

As anticipated in Section II, an essential prerequisite to an effective study of the elastic properties of crystals at high pressure, at the *ab initio* level, is a correct description of the pressure-volume relation. In order to establish such a connection, we optimize the cell volume in presence of an external pre-stress, in the form of an hydrostatic pressure (see equation 3), following the procedure described in Section II A.

The computed P-V relations for pyrope (up to 60 GPa), grossular (up to 60 GPa) and andradite (up to 40 GPa) are reported as continuous lines in Figure 1 and compared with accurate experimental data. Since pyrope is considered to be a major constituent in the Earth's upper mantle and transition zone, its equation of state has been extensively studied experimentally in the last 40 years with different techniques such as ultrasonic,

Brillouin scattering and X-ray diffraction.[167–176] In the lower panel of Figure 1, as an experimental reference, we consider the X-ray diffraction study on a pure synthetic pyrope single-crystal, up to 33 GPa, that Zhang *et al.* performed in 1998, where a complete review of previous studies is also reported.[165] They concluded that most previous measurements at $P > 10$ GPa were performed under nonhydrostatic conditions that severely biased the corresponding outcomes. In a subsequent study, Zhang *et al.* reported about accurate X-ray diffraction measurements on the compressibility of, among other silicate garnets, synthetic grossular and andradite, up to 12 GPa and 14 GPa, respectively.[166] These experimental values are reported in the upper and middle panels of Figure 1. For andradite, we also report the values obtained with a Brillouin scattering experiment, up to 11 GPa, by Jiang *et al.* in 2004.[107] A satisfactory agreement between computed and experimental P-V relations is obtained for the three garnets, as clearly seen from Figure 1. This reliable description of the P-V relation does represent an essential prerequisite for what follows.

Given the excellent description obtained with the analytical stress tensor approach, one may wonder about the accuracy that could be reached in computing the P-V relation by following the alternative scheme, based on the EOS, described in Section II B. In Table I we report the deviations from such analytical reference of the volumes deduced from various EOSs (Murnaghan, Birch-Murnaghan, Poirier-Tarantola and Vinet, see Appendix A for their explicit functional form), as a function of pressure, for pyrope, P, grossular, G, and andradite, A. For comparison, the analytical values of Figure 1 are also reported. Before discussing into some detail how different EOSs describe the P-V relation, let us point out that they have been obtained by fitting energy/volume points with the most compressed volume corresponding to a pressure of about 17 GPa. This means that values in Table I below and above 17 GPa have been obtained by interpolation and extrapolation, respectively. These two regions are separated by a horizontal line in the table. As a first consideration, we can see how the four different EOSs are providing exactly the same volumes (quite close to the analytical ones) in the interpolation region, that is for $P \leq 12$ GPa in the table. When we consider the extrapolation region, the four EOSs slightly deviates from each other; overall, all of them remain quite close to the analytical reference, with maximum differences of 0.4 % for pyrope, at 60 GPa, with the Poirier-Tarantola logarithmic EOS, 0.6 % for grossular, at 60 GPa, with the Murnaghan EOS and 0.5 % for andradite, at 40 GPa, with the Murnaghan EOS. Since differences among the four EOSs are very small, it is difficult to tell which one is providing the best description as regards the P-V relation of this family of garnets: Birch-Murnaghan for pyrope, Vinet for grossular and Poirier-Tarantola for andradite. All of them are essentially providing an acceptable de-

TABLE I. Volume V (in Å^3) of the primitive cell and bulk modulus K (in GPa) as a function of pressure P (in GPa) for pyrope, P, grossular, G and andradite, A. Computed values obtained with the procedure described in Sections II A and II C (Cal.) are reported in the first column of each property. Deviations from such reference values of those deduced from various equations of state: Murnaghan, M, Birch-Murnaghan, BM, Poirier-Tarantola, PT and Vinet, V are also reported; the horizontal lines separate interpolation from extrapolation regions for the EOSs.

	P	V (Å^3)					K (GPa)				
		Cal.	Fitted to EOS				Cal.	Fitted to EOS			
			M	BM	PT	V		M	BM	PT	V
P	0	770.0	0.5	0.5	0.5	0.5	171	0	1	1	1
	4	753.0	0.5	0.5	0.5	0.5	188	-1	-1	0	0
	8	737.7	0.5	0.5	0.5	0.5	203	0	0	0	0
	12	723.7	0.6	0.6	0.6	0.6	220	-1	-1	-2	-2
	20	699.4	0.7	0.5	0.3	0.4	251	1	-2	-5	-3
	30	673.9	0.8	0.2	-0.2	0.0	289	3	-4	-9	-6
	40	652.3	1.1	0.0	-1.0	-0.5	326	6	-5	-13	-9
	60	617.1	2.0	-0.6	-2.6	-2.7	399	13	-8	-24	-17
G	0	852.4	0.4	0.4	0.4	0.4	171	0	0	0	0
	4	833.6	0.3	0.4	0.4	0.4	187	0	0	0	0
	8	816.7	0.3	0.3	0.4	0.3	203	0	0	0	0
	12	800.6	1.1	1.1	1.1	1.1	219	0	0	-1	0
	20	773.8	1.2	1.2	0.8	0.9	250	2	-1	-3	-2
	30	745.6	1.4	0.8	0.2	0.5	288	5	-1	-7	-4
	40	721.6	2.0	0.7	-0.4	0.1	325	11	-1	-10	-6
	60	681.6	4.3	1.5	-1.0	0.2	396	20	-1	-18	-11
A	0	903.8	0.1	0.1	0.1	0.1	152	0	0	1	1
	4	881.5	0.1	0.1	0.1	0.1	169	0	1	1	1
	8	861.9	0.1	0.2	0.2	0.2	187	0	0	-1	-1
	12	844.6	0.0	-0.1	-0.1	-0.1	204	0	-1	-2	-1
	20	812.8	1.8	1.4	1.1	1.3	234	5	1	-2	0
	30	781.1	2.7	2.8	0.8	1.3	273	9	2	-6	-2
	40	754.8	3.6	1.9	0.1	1.0	311	15	2	-10	-4

scription of the compressibility of these minerals. As we shall comment below, this is no more the case when the bulk modulus dependence from pressure, K-P, is considered.

Following the procedure described in Section II C, we have computed the elastic stiffness constants B_{vu} of pyrope and grossular up to 60 GPa and those of andradite up to 40 GPa. The three independent constants, B_{11}, B_{12} and B_{44}, are reported in Figure 2 as black lines for andradite (top panel), grossular (middle panel) and pyrope (lower panel); their trend with respect to pressure is quite similar for the three garnets and it is quasi-linear, with B_{12} showing a slightly more linear behavior than
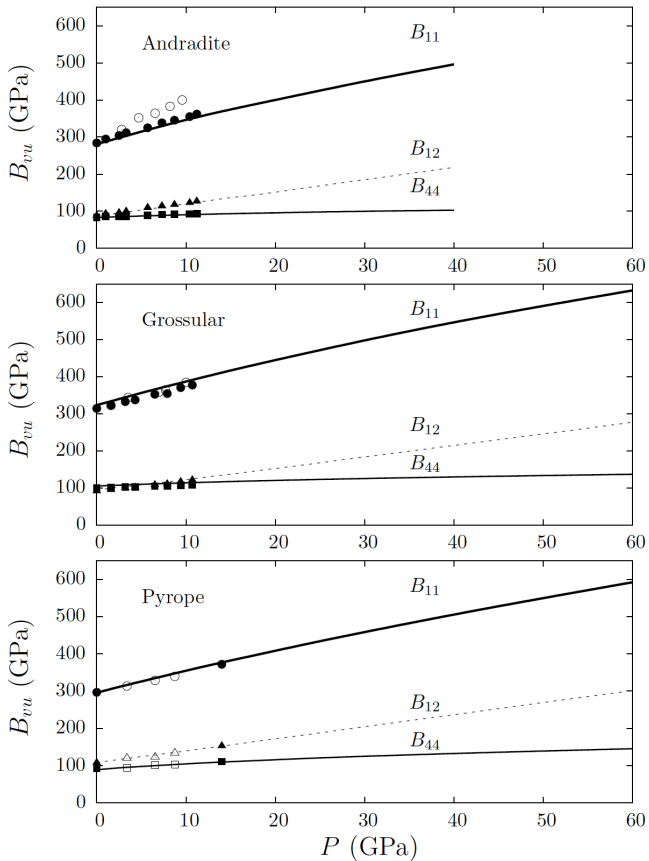
FIG. 2. Elastic stiffness constants B_{vu} of pyrope (lower panel), grossular (middle panel) and andradite (upper panel), as a function of pressure P. Black lines represent computed values. For pyrope, two experimental datasets are reported: one by Sinogeikin and Bass[105] (filled symbols) and one by Conrad et al.[106] (empty symbols). For grossular, the results by Jiang et al.[100] are reported (filled symbols) as well as those by Conrad et al.[106] (empty symbols) for the B_{11} constant. For andradite, experimental values by Jiang et al.[107] (filled symbols) are given along with those by Conrad et al.[106] (empty symbols) for the B_{11} constant. All experimental values are obtained from Brillouin scattering measurements.

B_{11} and B_{44}. In Figure 2 we also report available experimental data, obtained from various Brillouin scattering measurements.

For pyrope, two experimental determinations of the elastic constants at high pressure have been performed: one by Sinogeikin and Bass[105] who reported values at ambient pressure and at $P = 14$ GPa (given as filled symbols in the figure) and one by Conrad et al.[106] who reported values at three different pressures (given as empty symbols in the figure). From the analysis of the lower panel of Figure 2 the following considerations can be made: i) the two experimental datasets agree relatively well with each other; ii) as already noticed in our previous study of the elastic constants of silicate garnets at ambient pressure,[101] the absolute computed values of B_{vu} at $P = 0$ GPa are found in excellent agreement with the mea-

sured ones; iii) the computed pressure dependence of the elastic stiffness constants satisfactorily matches available experimental data in the low-pressure regime.

Also for grossular, two experiments are available to compare with: the results by Jiang et al.,[100] that refer to a 87 % grossular-rich garnet, are reported as filled symbols in the middle panel of Figure 2; they reported elastic constants at 8 different pressures up to 11 GPa. The values obtained by Conrad et al.[106] at 5 different pressures up to 10 GPa for the B_{11} constant are also reported as empty symbols; for this latter study, that is less accurate than the former one (2 crystal directions were measured at each pressure for the latter with respect to 36 in the former), we do not report the values for B_{12} and B_{44} for sake of clarity. We observe that: i) the two experiments give a similar description of B_{11} while the two remaining constants are described very differently (not shown in the figure), as previously discussed by Jiang et al.;[100] ii) the absolute values of the elastic constants at ambient pressure agree with the experiments as regards B_{12} and B_{44} while B_{11} is slightly overestimated in this case (let us recall that the experiment by Jiang et al. was performed on a 87 % grossular-rich garnet with 9 % of andradite which exhibits lower elastic constants than grossular); iii) the pressure dependence of all elastic constants nicely compares with the experimental behavior; in particular, the low-pressure crossing of B_{12} and B_{44} is perfectly reproduced.

For andradite, two experimental datasets are available: Jiang et al.[107] reported values at 9 pressures up to 11 GPa (filled symbols in the figure). Again, for B_{11} we also report, as empty symbols, the less accurate results by Conrad et al.[106] who measured the elastic constants at 5 pressures up to 10 GPa. Some considerations: i) the two experiments describe a very different pressure dependence of the elastic constants (shown for B_{11}, not for the other constants just for clarity sake); ii) both the absolute values at ambient pressure and the pressure dependence of computed constants are in good agreement with data by Jiang et al. and, consequently, significantly deviate from those by Conrad et al.; iii) Given the reliable description of the pressure dependence of computed elastic constants of pyrope and grossular, our results for andradite confirm the higher accuracy of the measurements by Jiang et al. with respect to those by Conrad et al..

The computed values for the elastic stiffness constants as a function of pressure are explicitly reported in Table II for pyrope, grossular and andradite. In the same table, we also report some elastic properties of isotropic polycrystalline aggregates, as computed via the Voigt-Reuss-Hill averaging scheme illustrated in Section II C: bulk modulus K, shear modulus $\overline{G}$, Young modulus E, Poisson's ratio σ and the anisotropy factor A. In particular, from the pressure dependence of the computed bulk modulus K, its first derivative K' can be deduced and compared with experimental determinations obtained from various EOSs (see below for such a comparison).

TABLE II. Elastic properties of pyrope, grossular and andradite as a function of pressure P (GPa). Elastic constants B_{vu}, bulk modulus K, shear modulus $\overline{G}$ and Young modulus E are expressed in GPa, Poisson's ratio σ is dimensionless and the anisotropy factor A is expressed in %. All these properties are defined in Section II C.

	Pyrope								Grossular								Andradite							
P	B_{11}	B_{12}	B_{44}	K	$\overline{G}$	E	σ	A	B_{11}	B_{12}	B_{44}	K	$\overline{G}$	E	σ	A	B_{11}	B_{12}	B_{44}	K	$\overline{G}$	E	σ	A
0	296	109	89	171	91	231	0.27	-3.0	323	95	105	171	109	269	0.24	-5.6	281	87	83	152	88	222	0.26	-10.0
4	320	121	96	188	98	250	0.28	-2.2	350	106	109	187	114	284	0.25	-7.4	308	100	86	169	93	236	0.27	-11.7
8	344	133	102	203	103	265	0.28	-2.0	375	117	112	203	119	298	0.26	-9.1	334	113	89	187	97	248	0.28	-12.9
12	366	146	107	220	108	279	0.29	-1.6	399	129	115	219	123	311	0.26	-10.0	358	126	92	204	101	259	0.29	-13.4
20	409	172	116	251	117	304	0.30	-1.2	445	153	120	250	130	333	0.28	-11.7	400	152	96	234	106	277	0.30	-14.0
30	459	205	125	289	126	330	0.31	-0.9	498	184	126	288	137	356	0.29	-12.5	450	185	100	273	112	295	0.32	-14.4
40	505	237	133	326	133	352	0.32	-0.4	547	215	130	325	143	375	0.31	-13.2	496	218	103	311	116	309	0.33	-14.5
60	592	302	146	399	145	389	0.34	+0.3	633	277	137	396	152	404	0.33	-13.0								

Among the elastic properties reported in the table, the elastic anisotropy index A is particularly interesting. In our previous investigation of the elastic properties of six silicate garnet end-members at ambient pressure, we have sorted them in terms of increasing anisotropy: spessartine and pyrope are the more isotropic, grossular and almandine show an intermediate anisotropy, and andradite and uvarovite are characterized by the largest elastic anisotropy.[101] The same relative behavior is observed in the first row ($P = 0$ GPa) of Table II with anisotropies of -3.0 %, -5.6 % and -10 % for pyrope, grossular and andradite, respectively. In this respect, Table II tells us how such elastic anisotropy is affected by pressure. Interestingly, pyrope is found to further decrease its already low anisotropy down to 0.3 % at 60 GPa while the other two garnets show an increasing anisotropy, more so for grossular than for andradite.

The values obtained for the bulk modulus K from the explicit calculation of the elastic constants, as a function of pressure, are also reported (column "Cal.") in Table I, along with the deviations from such values of the bulk moduli deduced from the four EOSs (Murnaghan, Birch-Murnaghan, Poirier-Tarantola and Vinet) described in Appendix A. As already discussed for the P-V relation above, also for the bulk modulus K, as far as the interpolation region $P < 17$ GPa is considered, the four EOSs provide similar values of K to each other and to the computed reference from the elastic constants. In particular, this remarkable matching of computed bulk moduli from the elastic constants and from the EOS-formalism is a nice evidence of the high numerical precision of all the algorithms involved in the simulation.

At variance with what previously observed for the P-V relation, when the bulk modulus is considered, as soon as the extrapolation region $P > 17$ GPa is reached, the descriptions provided by the different EOSs rapidly diverge from each other with differences as large as 10 % for pyrope and grossular at 60 GPa and 8 % for andradite at 40 GPa. From inspection of Table I, we can deduce that the third-order logarithmic Poirier-Tarantola EOS is providing the lowest values for K at high pressure (the poor description provided by this EOS has already been described by Pavese[177] who concluded that fourth-order terms are necessary for correcting it), the third-order Murnaghan's one the highest while Birch-Murnaghan' and Vinet' give intermediate values. By comparing with the bulk modulus values computed from the elastic stiffness constants at each pressure, we can clearly observe that the closest agreement is obtained with the third-order Birch-Murnaghan EOS, more so for grossular and andradite than for pyrope for which none of the four EOSs is providing an entirely satisfactory agreement.

From an experimental point of view, a lot of X-ray diffraction studies focused on measuring isothermal equations of state of rock-forming minerals in order to determine their bulk modulus K_0 and its pressure derivative K_0' (see the comprehensive work by Knittle[99] for a review on the topic). If at ambient pressure, different experimental determinations of K_0, agree relatively well to each other, this is not the case at high pressures where disagreements up to 50 % are commonly reported as regards K_0'. As noted by Jiang et $al.$, the magnitude of these discrepancies is such that a reliable geological interpretation of seismic data becomes unlikely on these grounds.[100] The spread among existing experimental de-

TABLE III. Bulk modulus pressure derivative K_0' of pyrope, grossular and andradite garnets as computed in the present study and determined in previous experimental studies.

Pyrope		Grossular		Andradite	
This study (2014)	4.1	This study (2014)	4.0	This study (2014)	4.4
Zou et al.[176] (2012)	4.4 - 4.6	Gwanmesia et al.[182] (2013)	4.5	Jiang et al.[107] (2004)	4.7
Gwanmesia et al.[175] (2006)	3.9	Gréaux et al.[183] (2011)	4.0 - 4.3	Wang and Ji[181] (2001)	4.7
Sinogeikin and Bass[105] (2000)	4.1	Kono et al.[184] (2010)	4.4	Conrad et al.[106] (1999)	5.8
Chen et al.[174] (1999)	5.3	Jiang et al.[100] (2004)	3.8		
Conrad et al.[106] (1999)	3.2	Wang and Ji[181] (2001)	5.9		
Zhang et al.[165] (1998)	4.4	Conrad et al.[106] (1999)	5.5		
Leger et al.[173] (1990)	3.8	Olijnyk et al.[180] (1991)	6.2		
Webb[169] (1989)	4.9	Weaver et al.[185] (1976)	4.5		
Levien et al.[186] (1979)	4.5				
Sato et al.[178] (1978)	1.8				
Bonczar and Graham[167] (1977)	4.7				
Takahashi and Liu[179] (1970)	5.4				

terminations of K_0' is documented in Table III where we also report our computed values for pyrope, grossular and andradite.

For pyrope, even without considering the oldest works, where discrepancies as large as 200 % were reported (1.8 for Sato et al.[178] and 5.4 for Takahashi and Liu[179]), also among the most recent studies differences as large as 65 % are reported (compare 5.3 by Chen et al.[174] with 3.2 by Conrad et al.[106]). The accurate work by Sinogeikin and Bass in 2000 gives a value of 4.1 which is found to be in perfect agreement with our present simulations. For grossular, K_0' values are spread from 6.2, as obtained by Olijnyk et al.[180] in 1991, to 3.8 by Jiang et al.[100] in 2004 (a difference of 63 %). In this case, our computed value is 4.0, whereas almost all the experimental determinations are a bit higher. For andradite, less experimental determinations are reported, with a maximum deviation from each others of 23 %. The two most recent studies (Jiang et al.[107] in 2004 and Wang and Ji[181] in 2001), both report a value of 4.7 while our calculated value is 4.4.

V. CONCLUSIONS

A theoretical scheme, as implemented in the CRYSTAL program, has been presented which allows for computing a variety of elastic properties under pressure of crystalline materials of any symmetry, at the *ab initio* level. The technique consists in optimizing the cell volume at a given pressure by means of the analytical calculation of the corresponding stress tensor and then automatically applying to the lattice all the needed deformations in order to compute the independent elastic constants which are pressure-corrected according to their Eulerian strain formulation.

This strategy has been applied to the investigation of high-pressure elastic properties of three rock-forming minerals such as pyrope, grossular and andradite, for which experimental data to compare with are available, even if only in the $P \leq 11$ GPa pressure range. The theoretical description of both the pressure-volume relation and the pressure dependence of elastic constants has been documented to be extremely reliable for this class of materials. Among other elastic indices, the anisotropy index has been found to decrease to very small values for pyrope and increase to similar values for grossular and andradite, as a function of pressure.

Both theoretically and experimentally, the high-pressure elastic behavior of crystals has often been deduced by fitting energy-volume, or pressure-volume data to given equations of state. Four different analytical expressions of equations of state have been considered, among the most popular proposals in the literature, and their descriptions of high-pressure elastic properties discussed. All of them are providing fairly good pressure-volume relations whereas large discrepancies between each other have been reported as regards the pressure dependence of the bulk modulus, the third-order Birch-

Murnaghan equation giving somehow the best description.

Appendix A: Equations of State: Functional Form

The four EOSs implemented in the CRYSTAL14 program and discussed in this paper are here reviewed; in particular, explicit expressions are provided for the bulk modulus dependence on volume (and thus on pressure, from the P-V relation) that are of interest for the study of elastic properties of materials under pressure. For convenience, let us introduce the dimensionless parameters $v = (V_0/V)^{1/3}$, $u = v^{-1}$ and $x = \ln(V_0/V)$ with V_0 equilibrium volume. The $E(V)$ functional form proposed by Murnaghan in 1944 reads as:[136]

$$E(V) = E_0 + \frac{K_0 V}{K_0'} \left(\frac{v^{3K_0'}}{K_0' - 1} + 1 \right) - \frac{K_0 V_0}{K_0' - 1} , \quad \text{(A1)}$$

where E_0 is the equilibrium energy. From $P = -(\partial E/\partial V)_S$ we get

$$P(V) = \frac{K_0}{K_0'} \left(v^{3K_0'} - 1 \right) . \quad \text{(A2)}$$

Since, by definition, $K(V) = V(\partial^2 E/\partial V^2)_{T,S}$, by differentiating equation (A1) twice with respect to the volume V, one obtains

$$K(V) = K_0 v^{3K_0'} . \quad \text{(A3)}$$

The previous EOS is often used for $0 < P < K_0/2$. The $E(V)$ form of the third-order isothermal EOS, proposed by Birch in 1947, reads like:[137]

$$E(V) = E_0 + \frac{9V_0 K_0}{16} \left[K_0' \left(v^2 - 1 \right)^3 + \left(v^2 - 1 \right)^2 \left(6 - 4v^2 \right) \right]$$

By differentiating the previous expression with respect to the volume, the corresponding $P(V)$ expression is obtained:

$$P(V) = \frac{3K_0}{2} \left(v^7 - v^5 \right) \left[1 + \frac{3}{4}(K_0' - 4) \left(v^2 - 1 \right) \right] \quad \text{(A4)}$$

The bulk modulus dependence on volume in this case becomes:

$$K(V) = \frac{K_0(4 - K_0')}{8} \left(42v^7 - 27v^9 - 15v^5 \right) - \frac{K_0}{2} \left(5v^5 - 7v^7 \right)$$

The $E(V)$ expression of the logarithmic Poirier-Tarantola EOS, as proposed in 1998 is:[141]

$$E(V) = E_0 + \frac{K_0 V_0}{2}x^2 + \frac{K_0 V_0}{6}x^3 \left(K_0' - 2 \right) . \quad \text{(A5)}$$

The corresponding $P(V)$ expression is:

$$P(V) = K_0 v^3 \left[x + \frac{\left(K_0' - 2 \right)}{2} x^2 \right] . \quad \text{(A6)}$$

The bulk modulus dependence on volume becomes:

$$K(V) = K_0 v^3 \left[1 + \left(K_0' - 1 \right) x + \frac{\left(K_0' - 2 \right)}{2} x^2 \right] . \quad \text{(A7)}$$

The $E(V)$ functional form of the exponential EOS by Vinet (1987) reads as:

$$E(V) = E_0 - \frac{4K_0 V_0}{\left(K_0' - 1 \right)^2} \left[1 - \frac{3}{2}(K_0' - 1)(1 - u) \right] \times$$
$$\times e^{\frac{3}{2}\left(K_0' - 1 \right)(1 - u)} \quad \text{(A8)}$$

The above expression is also known as bonding energy relation. The corresponding $P(V)$ expression becomes

$$P(V) = 3K_0 \frac{1 - u}{u^2} e^{\frac{3}{2}\left(K_0' - 1 \right)(1 - u)} , \quad \text{(A9)}$$

which is exact for a harmonic crystal with $K_0' = 1$. The bulk modulus dependence on volume is:

$$K(V) = K_0 v^2 e^{\frac{3}{2}\left(K_0' - 1 \right)(1 - u)} \times$$
$$\times \left\{ 2 + u \left[\frac{3}{2} \left(K_0' - 1 \right) - 1 \right] - \frac{3}{2} \left(K_0' - 1 \right) u^2 \right\}$$

The Vinet EOS is found to be more realistic than the Murnaghan and Birch ones for large compressions, $P \gg K_0/2$.

[94] T. S. Duffy and D. L. Anderson, J. Geophys. Res. **94**, 1895 (1989).

[95] M. J. P. Musgrave, *Crystal Acoustics* (Holden-Day, San Francisco, California, 1970).

[96] B. A. Auld, *Acoustic Fields and Waves in Solids* (Krieger Publishing Company, Malabar, Florida, 1973).

[97] B. B. Karki, L. Stixrude, and R. M. Wentzcovitch, Rev. Geophys. **39**, 507 (2001).

[98] G. Ottonello, B. Civalleri, J. Ganguly, W. F. Perger, D. Belmonte, and M. Vetuschi Zuccolini, Am. Mineral. **95**, 563 (2010).

[99] E. Knittle, in *A Handbook of Physical Constants: Mineral Physics and Crystallography*, edited by T. J. Ahrens (AGU, Washington D. C., 1995), vol. 2, pp. 98–142.

[100] F. Jiang, S. Speziale, and T. S. Duffy, J. Geophys. Res. **109**, B10210 (2004).

[101] A. Erba, A. Mahmoud, R. Orlando, and R. Dovesi, Phys. Chem. Minerals **41**, 151 (2014).

[102] A. Erba, A. Mahmoud, R. Orlando, and R. Dovesi, Phys. Chem. Minerals **41**, 161 (2014).

[103] G. A. Novak and G. V. Gibbs, Am. Mineral. **56**, 791 (1971).

[104] P. C. Rickwood, M. Mathias, and J. C. Siebert, Contrib. Mineral. Petrol. **19**, 271 (1968).

[105] S. V. Sinogeikin and J. D. Bass, Phys. Earth Planet. Int. **120**, 43 (2000).

[106] P. G. Conrad, C.-S. Zha, H.-K. Mao, and R. J. Hemley, Am. Mineral. **84**, 374 (1999).

[107] F. Jiang, S. Speziale, S. R. Shieh, and T. S. Duffy, J. Phys.:Condens. Matter **16**, S1041 (2004).

[108] B. Winkler, M. T. Dove, and M. Leslie, Am. Mineral. **76**, 313 (1991).

[109] A. Pavese, Phys. Chem. Minerals **26**, 649 (1999).

[110] R. Mittal, S. L. Chaplot, and N. Choudhury, Phys. Rev. B **64**, 094302 (2001).

[111] L. Li and D. J. Weidner, J. Earth. Science **22**, 169 (2011).

[112] K. Kawai and T. Tsuchiya, J. Geophys. Res.: Solid Earth **117**, B02202 (2012).

[113] A. D. Becke, J. Chem. Phys. **98**, 5648 (1993).

[114] C. Lee, W. Yang, and R. G. Parr, Phys. Rev. B **37**, 785 (1988).

[115] M. Miao, Nature Chemistry **5**, 846 (2013).

[116] P. D'Arco, F. Freyria Fava, and V. R. S. R. Dovesi, J. Phys.: Condens. Matter **8**, 8815 (1996).

[117] R. Dovesi, M. De La Pierre, A. M. Ferrari, F. Pascale, L. Maschio, and C. M. Zicovich-Wilson, Am. Mineral. **96**, 1787 (2011).

[118] C. M. Zicovich-Wilson, F. J. Torres, F. Pascale, L. Valenzano, R. Orlando, and R. Dovesi, J. Comput. Chem. **29**, 2268 (2008).

[119] A. Meyer, F. Pascale, C. M. Zicovich-Wilson, and R. Dovesi, Int. J. Quantum Chem. **110**, 338 (2010).

[120] L. Valenzano, A. Meyer, R. Demichelis, B. Civalleri, and R. Dovesi, Phys. Chem. Minerals **36**, 415 (2009).

[121] L. Valenzano, F. Pascale, M. Ferrero, and R. Dovesi, Int. J. Quantum Chem. **110**, 416 (2010).

[122] V. Lacivita, P. D'Arco, R. Orlando, R. Dovesi, and A. Meyer, Phys. Chem. Minerals **40**, 781 (2013).

[123] R. Dovesi, R. Orlando, A. Erba, C. M. Zicovich-Wilson, B. Civalleri, S. Casassa, L. Maschio, M. Ferrabone, M. De la Pierre, P. D'Arco, et al., Int. J. Quantum Chem. (2014), in press.

[124] W. F. Perger, J. Criswell, B. Civalleri, and R. Dovesi, Comput. Phys. Commun. **180**, 1753 (2009).

[125] A. Erba, M. Ferrabone, J. Baima, R. Orlando, M. Rérat, and R. Dovesi, J. Chem. Phys. **138**, 054906 (2013).

[126] V. Lacivita, A. Erba, Y. Noël, R. Orlando, P. D'Arco, and R. Dovesi, J. Chem. Phys. **138**, 214706 (2013).

[127] A. Erba, K. E. El-Kelany, M. Ferrero, I. Baraille, and M. Rérat, Phys. Rev. B **88**, 035102 (2013).

[128] J. Baima, A. Erba, R. Orlando, M. Rérat, and R. Dovesi, J. Phys. Chem. C **117**, 12864 (2013).

[129] A. Erba and R. Dovesi, Phys. Rev. B **88**, 045121 (2013).

[130] A. Mahmoud, A. Erba, K. E. El-Kelany, M. Rérat, and R. Orlando, Phys. Rev. B **89**, 045103 (2014).

[131] K. Doll, R. Dovesi, and R. Orlando, Theor. Chem. Acc. **112**, 394 (2004).

[132] K. Doll, R. Dovesi, and R. Orlando, Theor. Chem. Acc. **115**, 354 (2006).

[133] K. Doll, Molecular Physics **108**, 223 (2010).

[134] A. B. Alchagirov, J. P. Perdew, J. C. Boettger, R. C. Albers, and C. Fiolhais, Phys. Rev. B **63**, 224115 (2001).

[135] R. E. Cohen, O. Gülseren, and R. J. Hemley, Am. Mineral. **85**, 338 (2000).

[136] F. D. Murnaghan, Proc. Natl. Acad. Sci. USA **30**, 244 (1944).

[137] F. Birch, Phys. Rev. **71**, 809 (1947).

[138] F. Birch, J. Geophys. Res. **83**, 1257 (1978).

[139] P. Vinet, J. Ferrante, J. R. Smith, and J. H. Rose, J. Phys. C **19**, 467 (1986).

[140] W. B. Holzapfel, Rep. Prog. Phys. **59**, 29 (1996).

[141] J.-P. Poirier and A. Tarantola, Physics of the Earth and Planetary Interiors **109**, 1 (1998).

[142] O. L. Anderson, *Equations of State of Solids for Geophysicists and Ceramic Science* (Oxford University Press, New York, 1995).

[143] T. S. Duffy and Y. Wang, Mineralogical Society of America Reviews in Mineralogy **37**, 425 (1998).

[144] J. Hama and K. Suito, J. Phys.: Cond. Matter **8**, 67 (1996).

[145] F. Stacey, B. Brennan, and R. Irvine, Geophys. Surveys **4**, 189 (1981).

[146] R. J. Angel, in *High-Pressure and High-Temperature Crystal Chemistry*, edited by R. Hazen and R. Downs (Mineralogical Society of America, 2000), pp. 35–59.

[147] B. B. Karki, G. J. Ackland, and J. Crain, J. Phys.: Cond. Matter **9**, 8579 (1997).

[148] J. Wang, J. Li, S. Yip, S. Phillpot, and D. Wolf, Phys. Rev. B **52**, 12627 (1995).

[149] D. C. Wallace, *Thermodynamics of Crystals* (Wiley, New York, USA, 1972).

[150] D. C. Wallace, Rev. Mod. Phys. **37**, 57 (1965).

[151] J. F. Nye, *Physical properties of crystals* (Oxford University Press, Oxford, 1957).

[152] R. Hill, J. Mech. Phys. Solids **11**, 357 (1963).

[153] B. B. Karki, L. Stixrude, S. J. Clark, M. C. Warren, G. J. Ackland, and J. Crain, Am. Mineral. **82**, 51 (1997).

[154] T. Tsuchiya and K. Kawamura, J. Chem. Phys. **114**, 10086 (2001).

[155] A. Authier and A. Zarembowitch, in *International Tables for Crystallography, Vol. D*, edited by A. Authier (Wiley, 2006), p. 72.

[156] F. Pascale, C. Zicovich-Wilson, R. Orlando, C. Roetti, P. Ugliengo, and R. Dovesi, J. Phys. Chem. B **109**, 6146 (2005).

[157] R. Dovesi, V. R. Saunders, C. Roetti, R. Orlando, C. M. Zicovich-Wilson, F. Pascale, K. Doll, N. M. Harrison, B. Civalleri, I. J. Bush, et al., *CRYSTAL14 User's Manual*, Università di Torino, Torino (2013), http://www.crystal.unito.it.

[158] K. Doll, Comput. Phys. Commun. **137**, 74 (2001).

[159] K. Doll, V. Saunders, and N. Harrison, Int. J. Quantum Chem. **82**, 1 (2001).

[160] B. Civalleri, P. D'Arco, R. Orlando, and R. D. V. R. Saunders, Chem. Phys. Lett. **348**, 131 (2001).

[161] C. G. Broyden, J. Inst. Math. Appl. **6**, 76 (1970).

[162] R. Fletcher, Comput. J **13**, 317 (1970).

[163] D. Goldfarb, Math. Comput. **24**, 23 (1970).

[164] D. F. Shanno, Math. Comput. **24**, 647 (1970).

[165] L. Zhang, H. Ahsbahs, and A. Kutoglu, Phys. Chem. Minerals **25**, 301 (1998).

[166] L. Zhang, H. Ahsbahs, A. Kutoglu, and C. A. Geiger, Phys. Chem. Minerals **27**, 52 (1999).

[167] L. J. Bonczar, E. K. Graham, and H. Wang, J. Geophys. Res. **82**, 2529 (1977).

[168] V. Babuška, J. Fiala, M. Kumazawa, I. Ohno, and Y. Sumino, Phys. Earth Planet. Int **16**, 157 (1978).

[169] S. L. Webb, Phys. Chem. Minerals **16**, 684 (1989).

[170] B. J. Leitner, D. J. Weidner, and R. C. Liebermann, Phys. Earth Planet. Int. **22**, 111 (1980).

[171] B. O'Neill, J. D. Bass, J. R. Smyth, and M. T. Vaughan, J. Geophys. Res. **94**, 17819 (1989).

[172] R. Hazen, R. Downs, P. Conrad, L. Finger, and T. Gasparik, Phys. Chem. Minerals **21**, 344 (1994).

[173] J. Leger, A. Redon, and C. Chateau, Phys. Chem. Minerals **17**, 161 (1990).

[174] G. Chen, J. A. Cooke Jr., G. D. Gwanmesia, and R. C. Liebermann, Am. Meneral. **84**, 384 (1999).

[175] G. D. Gwanmesia, J. Zhang, K. Darling, J. Kung, B. Li, L. Wang, D. Neuville, and R. C. Liebermann, Phys. Earth Planet. Inter. **155**, 179 (2006).

[176] Y. Zou, S. Gréaux, T. Irifune, M. L. Whitaker, T. Shinmei, and Y. Higo, Phys. Chem. Minerals **39**, 589 (2012).

[177] A. Pavese, Phys. Chem. Minerals **29**, 43 (2002), ISSN 0342-1791.

[178] Y. Sato, M. Akaogi, and S.-I. Akimoto, J. Geophys. Res. **83**, 335 (1978).

[179] T. Takahashi and L.-G. Liu, J. Geophys. Res. **75**, 5757 (1970).

[180] H. Olijnyk, E. Paris, C. A. Geiger, and G. A. Lager, J. Geophys. Res. **96**, 14313 (1991).

[181] Z. Wang and S. Ji, Am. Miner. **86**, 1209 (2001).

[182] G. D. Gwanmesia, L. Wang, A. Heady, and R. C. Liebermann, Phys. Earth Planet. Inter. (2013), doi: 10.1016/j.pepi.2013.09.010.

[183] S. Gréaux, Y. Kono, N. Nishiyama, T. Kunimoto, K. Wada, and T. Irifune, Phys. Chem. Minerals **38**, 85 (2011).

[184] Y. Kono, S. Gréaux, Y. Higo, H. Ohfuji, and T. Irifune, J. Earth Sci. **21**, 782 (2010).

[185] J. S. Weaver, T. Takahashi, and J. Bass, J. Geophys. Res. **81**, 2475 (1976).

[186] L. Levien, C. T. Prewitt, and D. J. Weidner, Am. Mineral. **64**, 805 (1979).

[94] T. S. Duffy and D. L. Anderson, J. Geophys. Res. **94**, 1895 (1989).

[95] M. J. P. Musgrave, *Crystal Acoustics* (Holden-Day, San Francisco, California, 1970).

[96] B. A. Auld, *Acoustic Fields and Waves in Solids* (Krieger Publishing Company, Malabar, Florida, 1973).

[97] B. B. Karki, L. Stixrude, and R. M. Wentzcovitch, Rev. Geophys. **39**, 507 (2001).

[98] G. Ottonello, B. Civalleri, J. Ganguly, W. F. Perger, D. Belmonte, and M. Vetuschi Zuccolini, Am. Mineral. **95**, 563 (2010).

[99] E. Knittle, in *A Handbook of Physical Constants: Mineral Physics and Crystallography*, edited by T. J. Ahrens (AGU, Washington D. C., 1995), vol. 2, pp. 98–142.

[100] F. Jiang, S. Speziale, and T. S. Duffy, J. Geophys. Res. **109**, B10210 (2004).

[101] A. Erba, A. Mahmoud, R. Orlando, and R. Dovesi, Phys. Chem. Minerals **41**, 151 (2014).

[102] A. Erba, A. Mahmoud, R. Orlando, and R. Dovesi, Phys. Chem. Minerals **41**, 161 (2014).

[103] G. A. Novak and G. V. Gibbs, Am. Mineral. **56**, 791 (1971).

[104] P. C. Rickwood, M. Mathias, and J. C. Siebert, Contrib. Mineral. Petrol. **19**, 271 (1968).

[105] S. V. Sinogeikin and J. D. Bass, Phys. Earth Planet. Int. **120**, 43 (2000).

[106] P. G. Conrad, C.-S. Zha, H.-K. Mao, and R. J. Hemley, Am. Mineral. **84**, 374 (1999).

[107] F. Jiang, S. Speziale, S. R. Shieh, and T. S. Duffy, J. Phys.:Condens. Matter **16**, S1041 (2004).

[108] B. Winkler, M. T. Dove, and M. Leslie, Am. Mineral. **76**, 313 (1991).

[109] A. Pavese, Phys. Chem. Minerals **26**, 649 (1999).

[110] R. Mittal, S. L. Chaplot, and N. Choudhury, Phys. Rev. B **64**, 094302 (2001).

[111] L. Li and D. J. Weidner, J. Earth. Science **22**, 169 (2011).

[112] K. Kawai and T. Tsuchiya, J. Geophys. Res.: Solid Earth **117**, B02202 (2012).

[113] A. D. Becke, J. Chem. Phys. **98**, 5648 (1993).

[114] C. Lee, W. Yang, and R. G. Parr, Phys. Rev. B **37**, 785 (1988).

[115] M. Miao, Nature Chemistry **5**, 846 (2013).

[116] P. D'Arco, F. Freyria Fava, and V. R. S. R. Dovesi, J. Phys.: Condens. Matter **8**, 8815 (1996).

[117] R. Dovesi, M. De La Pierre, A. M. Ferrari, F. Pascale, L. Maschio, and C. M. Zicovich-Wilson, Am. Mineral. **96**, 1787 (2011).

[118] C. M. Zicovich-Wilson, F. J. Torres, F. Pascale, L. Valenzano, R. Orlando, and R. Dovesi, J. Comput. Chem. **29**, 2268 (2008).

[119] A. Meyer, F. Pascale, C. M. Zicovich-Wilson, and R. Dovesi, Int. J. Quantum Chem. **110**, 338 (2010).

[120] L. Valenzano, A. Meyer, R. Demichelis, B. Civalleri, and R. Dovesi, Phys. Chem. Minerals **36**, 415 (2009).

[121] L. Valenzano, F. Pascale, M. Ferrero, and R. Dovesi, Int. J. Quantum Chem. **110**, 416 (2010).

[122] V. Lacivita, P. D'Arco, R. Orlando, R. Dovesi, and A. Meyer, Phys. Chem. Minerals **40**, 781 (2013).

[123] R. Dovesi, R. Orlando, A. Erba, C. M. Zicovich-Wilson, B. Civalleri, S. Casassa, L. Maschio, M. Ferrabone, M. De la Pierre, P. D'Arco, et al., Int. J. Quantum Chem. (2014), in press.

[124] W. F. Perger, J. Criswell, B. Civalleri, and R. Dovesi, Comput. Phys. Commun. **180**, 1753 (2009).

[125] A. Erba, M. Ferrabone, J. Baima, R. Orlando, M. Rérat, and R. Dovesi, J. Chem. Phys. **138**, 054906 (2013).

[126] V. Lacivita, A. Erba, Y. Noël, R. Orlando, P. D'Arco, and R. Dovesi, J. Chem. Phys. **138**, 214706 (2013).

[127] A. Erba, K. E. El-Kelany, M. Ferrero, I. Baraille, and M. Rérat, Phys. Rev. B **88**, 035102 (2013).

[128] J. Baima, A. Erba, R. Orlando, M. Rérat, and R. Dovesi, J. Phys. Chem. C **117**, 12864 (2013).

[129] A. Erba and R. Dovesi, Phys. Rev. B **88**, 045121 (2013).

[130] A. Mahmoud, A. Erba, K. E. El-Kelany, M. Rérat, and R. Orlando, Phys. Rev. B **89**, 045103 (2014).

[131] K. Doll, R. Dovesi, and R. Orlando, Theor. Chem. Acc. **112**, 394 (2004).

[132] K. Doll, R. Dovesi, and R. Orlando, Theor. Chem. Acc. **115**, 354 (2006).

[133] K. Doll, Molecular Physics **108**, 223 (2010).

[134] A. B. Alchagirov, J. P. Perdew, J. C. Boettger, R. C. Albers, and C. Fiolhais, Phys. Rev. B **63**, 224115 (2001).

[135] R. E. Cohen, O. Gülseren, and R. J. Hemley, Am. Mineral. **85**, 338 (2000).

[136] F. D. Murnaghan, Proc. Natl. Acad. Sci. USA **30**, 244 (1944).

[137] F. Birch, Phys. Rev. **71**, 809 (1947).

[138] F. Birch, J. Geophys. Res. **83**, 1257 (1978).

[139] P. Vinet, J. Ferrante, J. R. Smith, and J. H. Rose, J. Phys. C **19**, 467 (1986).

[140] W. B. Holzapfel, Rep. Prog. Phys. **59**, 29 (1996).

[141] J.-P. Poirier and A. Tarantola, Physics of the Earth and Planetary Interiors **109**, 1 (1998).

[142] O. L. Anderson, *Equations of State of Solids for Geophysicists and Ceramic Science* (Oxford University Press, New York, 1995).

[143] T. S. Duffy and Y. Wang, Mineralogical Society of America Reviews in Mineralogy **37**, 425 (1998).

[144] J. Hama and K. Suito, J. Phys.: Cond. Matter **8**, 67 (1996).

[145] F. Stacey, B. Brennan, and R. Irvine, Geophys. Surveys **4**, 189 (1981).

[146] R. J. Angel, in *High-Pressure and High-Temperature Crystal Chemistry*, edited by R. Hazen and R. Downs (Mineralogical Society of America, 2000), pp. 35–59.

[147] B. B. Karki, G. J. Ackland, and J. Crain, J. Phys.: Cond. Matter **9**, 8579 (1997).

[148] J. Wang, J. Li, S. Yip, S. Phillpot, and D. Wolf, Phys. Rev. B **52**, 12627 (1995).

[149] D. C. Wallace, *Thermodynamics of Crystals* (Wiley, New York, USA, 1972).

[150] D. C. Wallace, Rev. Mod. Phys. **37**, 57 (1965).

[151] J. F. Nye, *Physical properties of crystals* (Oxford University Press, Oxford, 1957).

[152] R. Hill, J. Mech. Phys. Solids **11**, 357 (1963).

[153] B. B. Karki, L. Stixrude, S. J. Clark, M. C. Warren, G. J. Ackland, and J. Crain, Am. Mineral. **82**, 51 (1997).

[154] T. Tsuchiya and K. Kawamura, J. Chem. Phys. **114**, 10086 (2001).

[155] A. Authier and A. Zarembowitch, in *International Tables for Crystallography, Vol. D*, edited by A. Authier (Wiley, 2006), p. 72.

[156] F. Pascale, C. Zicovich-Wilson, R. Orlando, C. Roetti, P. Ugliengo, and R. Dovesi, J. Phys. Chem. B **109**, 6146 (2005).

[157] R. Dovesi, V. R. Saunders, C. Roetti, R. Orlando, C. M. Zicovich-Wilson, F. Pascale, K. Doll, N. M. Harrison, B. Civalleri, I. J. Bush, et al., *CRYSTAL14 User's Manual*, Università di Torino, Torino (2013), http://www.crystal.unito.it.

[158] K. Doll, Comput. Phys. Commun. **137**, 74 (2001).

[159] K. Doll, V. Saunders, and N. Harrison, Int. J. Quantum Chem. **82**, 1 (2001).

[160] B. Civalleri, P. D'Arco, R. Orlando, and R. D. V. R. Saunders, Chem. Phys. Lett. **348**, 131 (2001).

[161] C. G. Broyden, J. Inst. Math. Appl. **6**, 76 (1970).

[162] R. Fletcher, Comput. J **13**, 317 (1970).

[163] D. Goldfarb, Math. Comput. **24**, 23 (1970).

[164] D. F. Shanno, Math. Comput. **24**, 647 (1970).

[165] L. Zhang, H. Ahsbahs, and A. Kutoglu, Phys. Chem. Minerals **25**, 301 (1998).

[166] L. Zhang, H. Ahsbahs, A. Kutoglu, and C. A. Geiger, Phys. Chem. Minerals **27**, 52 (1999).

[167] L. J. Bonczar, E. K. Graham, and H. Wang, J. Geophys. Res. **82**, 2529 (1977).

[168] V. Babuška, J. Fiala, M. Kumazawa, I. Ohno, and Y. Sumino, Phys. Earth Planet. Int **16**, 157 (1978).

[169] S. L. Webb, Phys. Chem. Minerals **16**, 684 (1989).

[170] B. J. Leitner, D. J. Weidner, and R. C. Liebermann, Phys. Earth Planet. Int. **22**, 111 (1980).

[171] B. O'Neill, J. D. Bass, J. R. Smyth, and M. T. Vaughan, J. Geophys. Res. **94**, 17819 (1989).

[172] R. Hazen, R. Downs, P. Conrad, L. Finger, and T. Gasparik, Phys. Chem. Minerals **21**, 344 (1994).

[173] J. Leger, A. Redon, and C. Chateau, Phys. Chem. Minerals **17**, 161 (1990).

[174] G. Chen, J. A. Cooke Jr., G. D. Gwanmesia, and R. C. Liebermann, Am. Meneral. **84**, 384 (1999).

[175] G. D. Gwanmesia, J. Zhang, K. Darling, J. Kung, B. Li, L. Wang, D. Neuville, and R. C. Liebermann, Phys. Earth Planet. Inter. **155**, 179 (2006).

[176] Y. Zou, S. Gréaux, T. Irifune, M. L. Whitaker, T. Shinmei, and Y. Higo, Phys. Chem. Minerals **39**, 589 (2012).

[177] A. Pavese, Phys. Chem. Minerals **29**, 43 (2002), ISSN 0342-1791.

[178] Y. Sato, M. Akaogi, and S.-I. Akimoto, J. Geophys. Res. **83**, 335 (1978).

[179] T. Takahashi and L.-G. Liu, J. Geophys. Res. **75**, 5757 (1970).

[180] H. Olijnyk, E. Paris, C. A. Geiger, and G. A. Lager, J. Geophys. Res. **96**, 14313 (1991).

[181] Z. Wang and S. Ji, Am. Miner. **86**, 1209 (2001).

[182] G. D. Gwanmesia, L. Wang, A. Heady, and R. C. Liebermann, Phys. Earth Planet. Inter. (2013), doi: 10.1016/j.pepi.2013.09.010.

[183] S. Gréaux, Y. Kono, N. Nishiyama, T. Kunimoto, K. Wada, and T. Irifune, Phys. Chem. Minerals **38**, 85 (2011).

[184] Y. Kono, S. Gréaux, Y. Higo, H. Ohfuji, and T. Irifune, J. Earth Sci. **21**, 782 (2010).

[185] J. S. Weaver, T. Takahashi, and J. Bass, J. Geophys. Res. **81**, 2475 (1976).

[186] L. Levien, C. T. Prewitt, and D. J. Weidner, Am. Mineral. **64**, 805 (1979).